Convolutional Neural Network-based Leakage Detection of Crude Oil Transmission Pipes

Anqi LI[1], Dongxu YE[1], Clarence W. DE SILVA[2], Max Q.-H. MENG[3]

(1. *Robotics, Perception and Artificial Intelligence Laboratory, Harbin Institute of Technology Shenzhen, Shenzhen* 518000;
2. *The University of British Columbia, Vancouver, BC, Canada V6T* 1Z4;
3. *The Chinese University of Hong Kong, Hong Kong*)

Abstract: Due to the rapid development in the petroleum industry, the leakage detection of crude oil transmission pipes has become an increasingly crucial issue. At present, oil plants at home and abroad mostly use manual inspection method for detection. This traditional method is not only inefficient but also labor-intensive. The present paper proposes a novel convolutional neural network (CNN) architecture for automatic leakage level assessment of crude oil transmission pipes. An experimental setup is developed, where a visible camera and a thermal imaging camera are used to collect image data and analyze various leakage conditions. Specifically, images are collected from various pipes with no leaking and different leaking states. Apart from images from existing pipelines, images are collected from the experimental setup with different types of joints to simulate leakage conditions in the real world. The main contributions of the present paper are, developing a convolutional neural network to classify the information in red-green-blue (RGB) and thermal images, development of the experimental setup, conducting leakage experiments, and analyzing the data using the developed approach. By successfully combining the two types of images, the proposed method is able to achieve a higher classification accuracy, compared to other methods that use RGB images or thermal images alone. Especially, compared with the method that uses thermal images only, the accuracy increases from about 91% to over 96%.

Key words: Pipeline Leakage, Convolutional Neural Network, RGB Images, Thermal Images, Data Fusion.

1 Introduction

Use of a pipeline network to transport oil over long distance has many advantages such as capability of handling high volumes of oil, high security, low cost, stable, and continuous transportation process. As a result, it has become the preferred choice of crude oil transportation. However, with the development of the pipeline transportation industry, pipeline leakage accidents have become somewhat common and serious, and is a problem that needs to be solved urgently. These accidents in pipelines can be caused by aging, wear, corrosion or deliberate human damage. Pipeline leakage not only causes economic losses and environmental pollution, but also leads to serious threat of human health and safety. Therefore, fast and automated leakage detection in pipelines is of great significance to reduce the occurrence of leakage accidents.

At present, leakage detection in the crude oil transportation industry is commonly done through human labor[1]. Human inspectors walk alongside the transmission pipelines to visually check the pipes and record the problems. This approach can be hazardous, slow, and inaccurate. To reduce the use of human labor and to improve the detection efficiency, automating the detection process has become a growing research area in recent years. Especially with the rapid development of deep learning technologies, many studies have used deep neural networks to conduct leakage detection. Sinha et al.[2] developed a fuzzy artificial neural network (ANN)-based pipeline reliability assessment method that uses eight pipeline parameters as the input variables. The output variable is the probability of failure. Francois Ayello et al. [3] proposed a pipeline risk assessment model based on Bayesian network, which can calculate

many types of risk, separately. The work of Giuseppe Acciani et al. [4] provided information for a neural network classifier by using the correlation coefficient between the x, y and z components of the simulated guided wave displacement reflected by the defect on a pipe, to evaluate the size of the defect on the pipe that is tested. Xiao Rui et al. [5] proposed an integrated leak detection method using acoustic signals based on wavelet transform and Support Vector Machine (SVM). In the work of Guzman et al. [6], a fuzzy logic-based model was designed to minimize the uncertainty of evaluating pipeline risks. In order to solve the problem of low efficiency of manual detection of drain pipes, Zijin Zhang et al. [7] proposed a defect detection method based on the Faster-RCNN algorithm. The most of such work focuses on using extracted features from images instead of the raw images. Based on the observation that the crude oil in the pipe is heated with steam before transportation, it is believed that thermal images will provide more information than RGB images[8-10]. Therefore, the present paper places more attention on combining RGB information and thermal information for leakage detection.

The present paper designs a CNN architecture[11] that extracts features from raw RGB and thermal images and processes the two types of images together. The innovation of the present neural network is the scoring method that incorporates both visible light information and thermal information.

This paper is organized into the following components: In the present section (Section 1) the background of the work is outlined. In Section 2, the underlying theoretical analysis and the basic structures of CNN are presented. In Section 3, the experimental system, the process of data acquisition, and image preprocessing are described. Then, in Section 4, the proposed CNN architecture is presented in detail. The obtained experimental results and their analysis are discussed in Section 5 of the paper. Concluding remarks are given in Section 6.

2 Theoretical Analysis

As an effective network structure, CNN has been widely used to solve practical problems including image recognition and classification. With the characteristics of local connection and weight sharing, the result of CNN is invariant with respect to small translation, scaling, and rotation disturbances in the input dataset. The structure of a CNN is generally a combination of the convolutional layer, the pooling layer[12] and the fully connected layer. The CNN model is trained using labeled data, by the backpropagation algorithm[13].

2.1 Convolutional layer

Convolutional layer, which contains multiple convolution kernels, is generally used to extract features from the input data. The input and the output of each convolutional layer are sets of arrays called feature maps. Each pixel in a feature map is the weighted average of the pixels in a small area of the input image, and the weight is determined by the value of the convolution kernel[14]. Convolution can be considered as a special linear operation. This operation can be expressed by,

$$X_j^{(l)} = F\left(\sum_{i=1}^{m} W^{(l)ij} \otimes X_i^{(l-1)} + b_j^{(l)}\right) \qquad (1)$$

where, l represents the l-th layer of the network, i represents the i-th input feature map, j represents the j-th output feature map, $X_j^{(l)}$ represents the j-th feature map of the l-th layer in the network, $W_{ij}^{(l)}$ represents the j-th kernel of the l-th layer in the network, $X_i^{(l-1)}$ represents the i-th feature map of the $(l-1)$-th layer of the network, $b_j^{(l)}$ represents the bias term of the l-th layer, $\otimes$ represents the convolution operation, and F represents the nonlinear activation function.

The activation function introduces nonlinearity into a neural network, which improves the nonlinear modeling ability of the network. Typical activation functions include sigmoid function, tanh function, and rectified linear unit (ReLu). ReLu function is adopted in the present paper because of its superior

performance compared to other activation functions. The ReLu is presented by the function,

$$F(x) = \max(0, x) \tag{2}$$

2.2 Pooling layer

In addition to the convolutional layer, another important part in a CNN is the pooling layer, which processes the feature mapping results obtained by the convolution operation. The pooling kernel commonly has different size, with a stride greater than 1. The pooling operation reduces the computation amount while retaining the main features of the data. It prevents over-fitting and improves the generalization ability of the CNN model effectively. Commonly, pooling operations include max pooling and average pooling. In many studies, max pooling is used, as given by,

$$y = \max h, wi, j = 1 x_{i,j} \tag{3}$$

where, h, w represent the height and the width of the pooling kernel, respectively, and $x_{i,j}$ represents the value of an overlap area between a feature map and a pooling kernel.

2.3 Fully connected layer

In the structure of CNN, the convolutional layer and the pooling layer perform feature extraction and dimensionality reduction, respectively. The fully connected layer and the softmax layer are followed at the end of the CNN, generally. These two types of layers integrate local information and map the extracted features into the "sample mark space", which plays the role of "classifier" in the network. The softmax layer often appears as the last layer of the CNN, after several fully connected layers. The number of nodes in the last layer is the same as the number of target (classified) categories. The softmax layer maps the output of the fully connected layer to the probability of each category (a value between 0-1). The probability can be calculated by,

$$P(t^i = j \mid x^{(i)}; W^{(L)}) = \left(\sum_{l=1}^{k} e^{(W_l^{(L)})^T \cdot x^{(i)}}\right)^{-1} \times \begin{bmatrix} e^{(W_1^{(L)})^T \cdot x^{(i)}} \\ e^{(W_2^{(L)})^T \cdot x^{(i)}} \\ \cdots \\ e^{(W_k^{(L)})^T \cdot x^{(i)}} \end{bmatrix} \tag{4}$$

where, $t^{(i)} \in \{1, 2, \ldots, k\}$ represents the number of target categories, $x^{(i)} \in R^n$ represents the output of the fully connected layer, and $W^{(L)}$ represents the weight of the softmax classifier.

2.4 Backpropagation algorithm

The working mechanism of CNN mainly consists of two parts: forward propagation and backward propagation. Forward propagation is used to predict the label of the input data, and the backward propagation updates parameters according to the value calculated by gradient function of the loss function, for each parameter.

Supervised learning is performed by CNN, using gradient descent. Although the formula for calculating the gradient is simple and straightforward, numerically solving this formula may require excessive computation, for example, for a deep network with millions of parameters. However, backpropagation algorithm takes the result of the loss function as input, and follows the chain rules to adopt a specific order of operations to calculate the gradient for each parameter. In the present paper, cross entropy loss function is adopted. The cost function is defined as,

$$J(W, b) = -\frac{1}{m}\left[\sum_{i=1}^{m}\left[y^{(i)} \cdot \log F_W(x^{(i)}) + (1 - y^{(i)}) \cdot \log(1 - F_W(x^{(i)}))\right]\right] \tag{5}$$

where, W represents the weight, $J(W, b)$ represents the loss function, m is the number of target categories, $y^{(i)}$ represents the real label of the i-th sample, and $F_w(x^{(i)})$ is the predicted value of the network.

After calculating the gradient, each parameter is updated along the direction of the gradient. In this way, the result of the loss function achieves the fastest decrease. The weight and the bias are updated according to,

$$W^{(j)} = W^{(j-1)} - \eta \frac{\partial}{\partial W} J(W,b)$$
$$b^{(j)} = b^{(j-1)} - \eta \frac{\partial}{\partial b} J(W,b) \quad (6)$$

where, η is the learning rate, and W and b represent the weight and the bias, respectively, which need to be updated along with the training process.

3 Data Acquisition

3.1 Experimental setup

Because of the joint defects and the stress concentration phenomenon, which is caused by a sudden cross sectional area change in a pipeline junction, leakage tends to occur in such area. In order to simulate the leakage conditions in the real world, an experimental platform is built in the lab. The experimental platform is designed with a fire hydrant with flange joint and a combined pipeline with two types of typical pipe joints: welded joint and threaded joint. For the purpose of obtaining temperature information and visible light information, NC160 thermal imaging camera (Shanghai Nobel) and X2 visible camera (Shenzhen electronic technology) are adopted in the present experimental setup. The developed experimental platform is shown in Fig. 1.

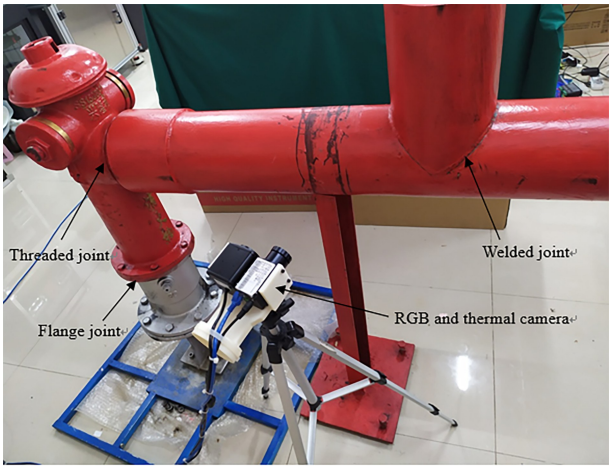

Fig. 1 Experimental platform.

3.2 Raw data acquisition

In order to verify the effectiveness of the proposed method, we collected 1010 RGB images and 1010 thermal images. Four leak conditions of the crude oil transmission pipelines are tested in the experiments, including the normal condition (no leak), and three leak conditions (large leak, moderate leak, minor leak). During the data collection process, the oil is poured at the pipe joints. The poured oil has different temperature and volume, which represent various leak conditions. Then the visible light camera and the thermal camera are placed at different poses to take the images simultaneously from different viewpoints. The experiment parameters are given in Table 1.

Table 1 Leakage classification and parameters.

Leakage type	Temperature of oil (℃)	Volume of oil (ml)	Amount of images
Large	70	10~15	172+172
Moderate	70	6~8	220+220
Minor	25	2~3	253+253
No	–	0	365+365

To extract the crude oil from wells and to improve the fluidity, the crude oil is commonly heated to around 60~80 degrees Celsius[15] using steam, in practice. A water bath heating device is used to heat oil to the specified temperature, to achieve this condition in the experiments. The oil temperature of a large leak and a moderate leak is controlled at around 70 degrees Celsius because of the large leakage amount that is present under these conditions, in the experiments. Considering that in a minor leak the area of leak is relatively small and the leakage volume is small as well, the oil temperature will be greatly affected by the temperature of the outer pipeline wall and the external environment. The leaked oil flows slowly along the pipe wall and cools rapidly in a few seconds, so the oil temperature is controlled at 25 degrees Celsius for the minor leak condition. In addition, the temperature of the outer pipeline wall is heated to around 35 degrees Celsius during the experiment. Because of the physical similarity between engine oil and crude oil, engine oil is used instead of crude oil in the experiments.

3.3 Data preprocessing

Many factors can influence the performance of the CNN model, of which the most important one is the size of the dataset. Due to the limited experimental setup, the dataset consisting of raw images is not large enough to train a robust CNN model. Therefore, an enhancement method is used to argument the original dataset to obtain sufficient number of images in the preprocessing stage. In the present paper, the data enhancement techniques include image up-and-down inversion, saturation adjustment, and contrast adjustment.

5050 RGB images and 5050 thermal images, of which 860×2 images correspond to large leak; 1100 ×2 images correspond to moderate leak; 1265×2 images correspond to minor leak, and 1825×2 images correspond to no leak, consist of the experimental dataset (×2 represents RGB and thermal images). In the present study, 60% of the dataset is used for the training of the CNN model, 20% of the dataset is used for the validation, and 20% is used for testing the trained network. The training dataset is used to train the CNN model by minimizing the error between the predicted value and the real value. The validation dataset is used to select the appropriate model by adjusting hyperparameters of the model, and the testing dataset is used to evaluate the generalization ability of the model and verify the validity of the method. Details of each category are shown in Table 2.

Table 2 The categories of the dataset.

Leakage type	Label	Train	Validate	Test	Total
Large	0	516	172	172	860
Moderate	1	660	220	220	1100
Minor	2	759	253	253	1265
No	3	1095	365	365	1825
Total	–	3030	1010	1010	5050

During the preprocessing stage, both RGB and thermal images are cropped into a size of 200×200. Then the RGB images and the thermal images are stitched together (RGB image on the left, thermal image on the right) to make a jointed image of size 200×400. The purpose of this step is to ensure that the RGB batch and the thermal batch are in one-to-one correspondence, and to be able to "fuse" the two types of images within the CNN.

4 CNN Model Structure Design

The present paper proposes a novel method based on CNN to automatically evaluate the leakage level of crude oil transmission pipelines. Compared to traditional methods, the present method has a strong ability for automated feature extraction, and only needs simple image data, which are taken from the exterior of the pipeline using an RGB camera and a thermal imaging camera. In the scoring stage of the proposed network, the features of the RGB image and the thermal image are combined together, forming a comprehensive standard to classify the leakage level corresponding to an input image. The flow chart of this process is shown in Fig. 2.

In order to realize the one-to-one correspondence of RGB images and thermal images in the initial stage, a batch with jointed images is produced. Then the jointed images are cropped into two images at the end of the batch-creating stage, and the cropped images (one RGB image and one thermal image) are given to different networks for training. This operation makes sure that each label accurately corresponds to RGB images and thermal images. Fig. 3 shows the detailed structure of the CNN.

Input images are convoluted by the convolution kernel F1 of size 7×7 with step 1×1, and the number of the output feature map is 64. The ReLu function is placed behind the output feature map of the convolutional layer. The purpose of this active function is to increase the nonlinearity of the network. Behind the convolutional layer is the max pooling layer with the pooling kernel of size 2×2, which reduces the dimension of the feature map and the parameters. This is followed by a sequential block of convolutional layers and max pooling layers. The differences be-

tween the blocks are the size and the number of convolutional kernels and max pooling kernels. Fig. 4 depicts the feature map extracted from each convolutional layer. Feature maps of the RGB image are given in the first row and the feature maps of the thermal image are given in the second row.

When all convolution and pooling operations are completed, the flattening operation is performed. The output after the flattening operation is used as the input to the fully connected layer. In the fully connected layer, the dropout[16] method is adopted to solve the overfitting problem (dropout is an operation that randomly discards the unit data of the fully connected layer in some proportion, during training). The number of neurons in the fully connected layer is 192, 96 and 4. In the scoring stage of the proposed network, the outputs from the RGB and the thermal network of the last fully connected layer are added to realize the fusion of the two types of information. The detailed parameters of the convolutional layers of the RGB network and the thermal network are give in Table 3.

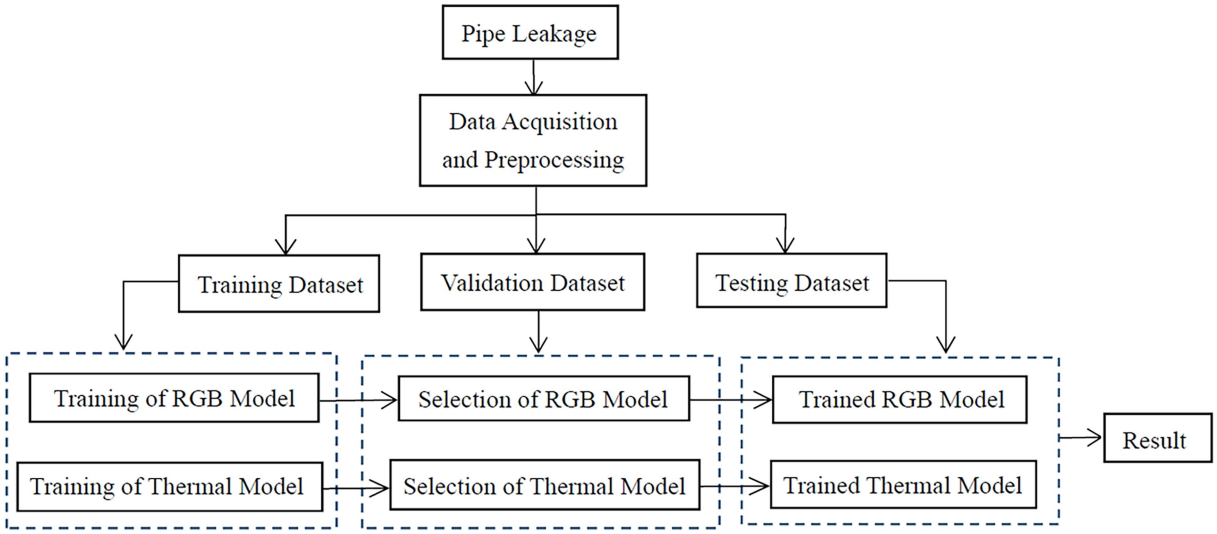

Fig. 2 Flow chart of the system.

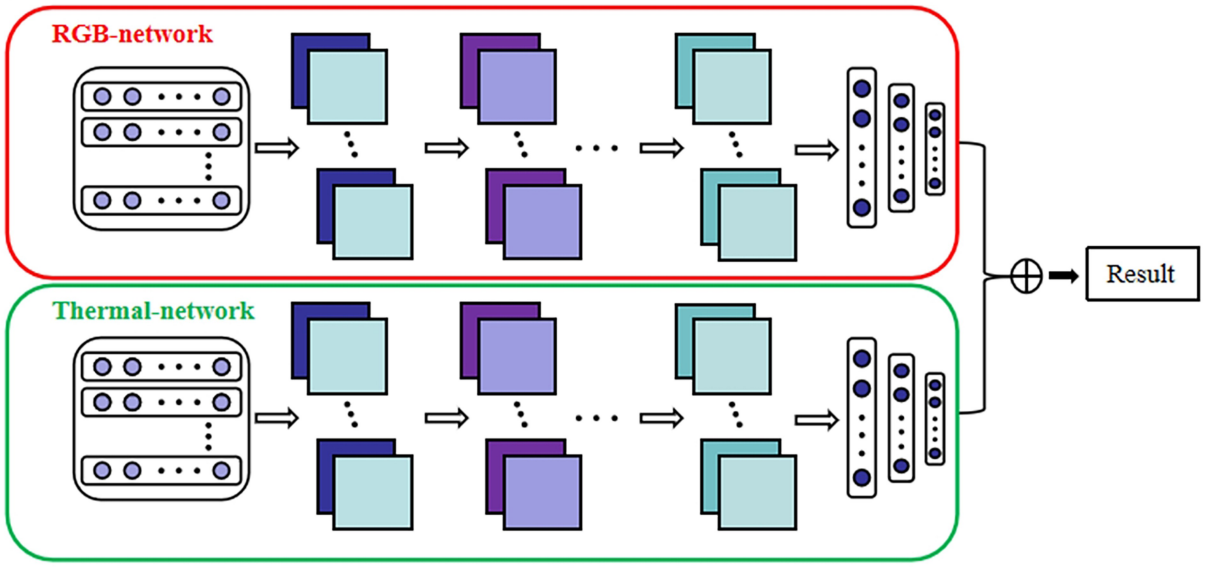

Fig. 3 The CNN structure.

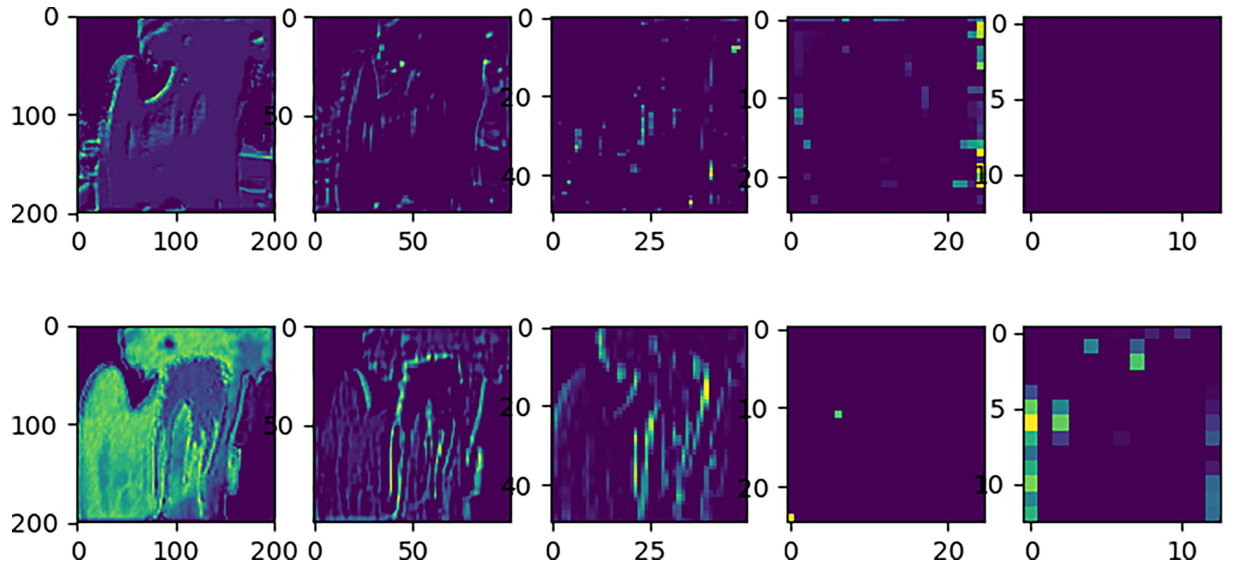

Fig. 4 Feature map.

Table 3 Parameters of the thermal and RGB network.

Thermal Network				RGB Network		
	Filters	Output map	Step	Filters	Output map	Step
Conv1_1	7×7	64	1×1	7×7	64	1×1
Conv1_2	7×7	64	1×1	7×7	64	1×1
Conv2_1	5×5	128	1×1	5×5	128	1×1
Conv2_2	5×5	128	1×1	5×5	128	1×1
Conv3	3×3	256	1×1	3×3	256	1×1
Conv4	3×3	256	1×1	3×3	512	1×1
Conv5_1	3×3	512	1×1	3×3	512	1×1
Conv5_2	3×3	512	1×1	–	–	–

5 Analysis of Experimental Data

Tensorflow 1.9.0 with the CUDA 9.0 and cudnn 7.3.1 libraries are adopted as the experimental environment. The graphics card used for training is a NVIDIA GTX 1080TI. During the training process, Adam is chosen as an adaptive learning rate optimizer to update each parameter. The RGB network and the thermal network are trained at the same time. In the output stage, the network adds the final output of the two types of networks as the final score of the input image, and this score is used for the classification of the leak level. The hyperparameters in the proposed CNN are adjusted according to the performance of the validation dataset. The learning rate is set to 0.0001, and the value of dropout is set to 0.5. The validation dataset plays an important role in determining the final CNN model. At the time of testing, the entire testing dataset is used to verify the performance the trained CNN model, and the classification accuracy of each leak condition is recorded.

In the task of pipeline leak assessment, an appropriate CNN model is selected through the training dataset and the verification dataset. Fig. 5 depicts the loss curve and accuracy curve in the training and the validation stages (Red curve represents the training process, and the blue curve represents the validation process). After the model selecton, the testing dataset is used to evaluate the performance of the CNN model.

Table 4 shows the accuracy of the method that uses the RGB images or the thermal images separately, and the accuracy of the RGB_Thermal fusion method. It can be seen that the thermal method has the lowest accuracy, only about 91%. The RGB_Thermal fusion method has the best performance, whose accuracy is nearly 97%.

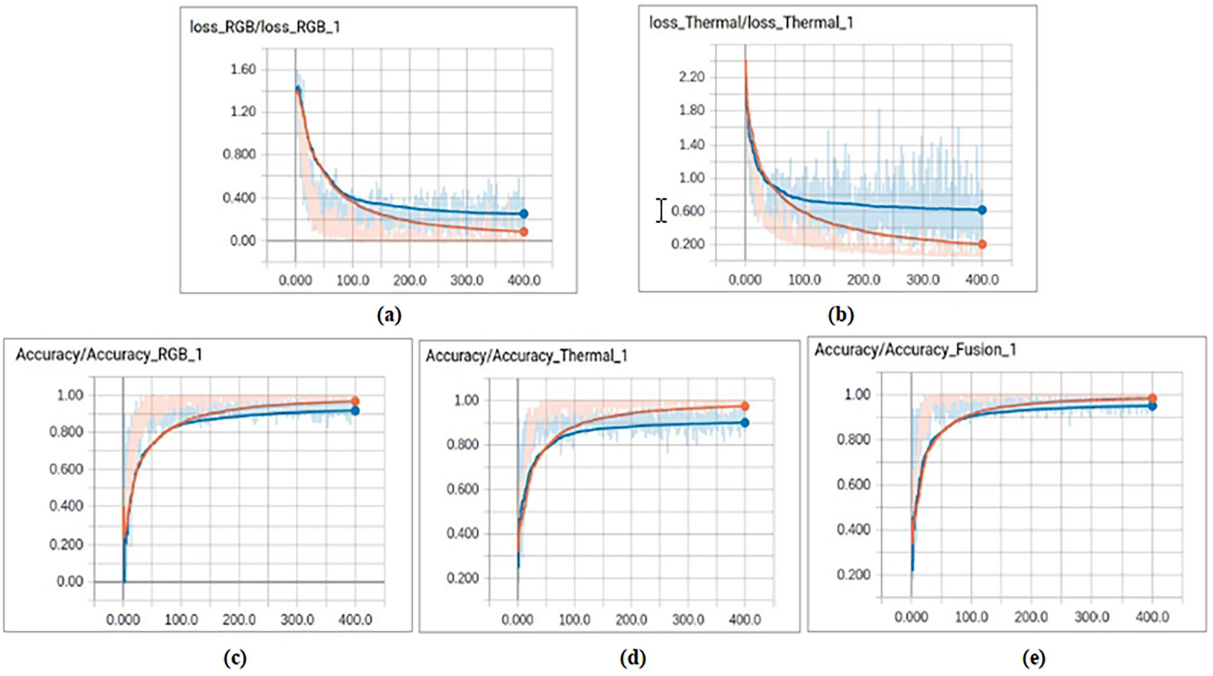

Fig. 5 (a) Loss of RGB network, (b) Loss of thermal network, (c) Accuracy of RGB network, (d) Accuracy of thermal network, (e) Accuracy of fusion method.

Table 4 Accuracy of the RGB, thermal, and fusion methods.

Method	RGB	Thermal	Fusion
Accuracy(%)	94.06	91.19	96.63

In order to verify the superiority of the RGB_Thermal fusion method for evaluation of the four leak conditions further, the accuracy of the four leak categories is determined, as shown in Fig. 6. It is observed that the accuracy of the RGB_Thermal fusion method in the moderator leak, minor leak, and no leak conditions is significantly higher than that of the RGB method or the thermal method. In the classification of the large leak images, the RGB_Thermal fusion method also reaches 95%. From a comprehensive perspective, the fusion method is more effective than the other two methods.

The next step is to demonstrate results of the four leakage conditions, by using the corresponding confusion matrix. As shown in Fig. 7, about 96% of the large leakage condition and 97% of the minor leakage condition are correctly classified by the proposed scheme. However, about 4% of the large leakage condition is misclassified as moderate leakage. About 95% of the moderate leakage and 98% of the no leakage condition are correctly detected by the method, but about 4% of the moderate leakage condition is misclassified as large leakage. This result verifies that the model has high accuracy and robustness, it can accurately classify the leakage level in crude oil transportation pipelines.

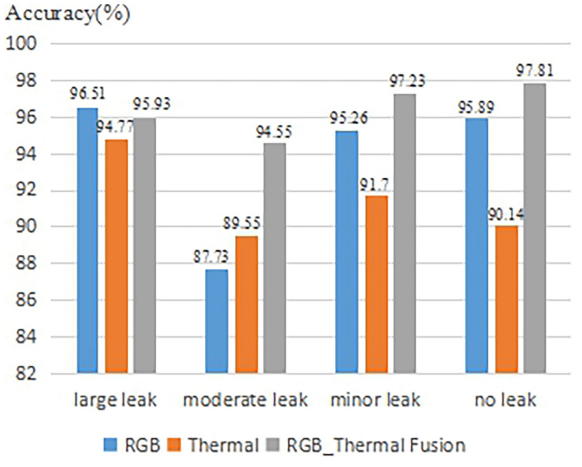

Fig. 6 Accuracy levels of four leakages using different methods.

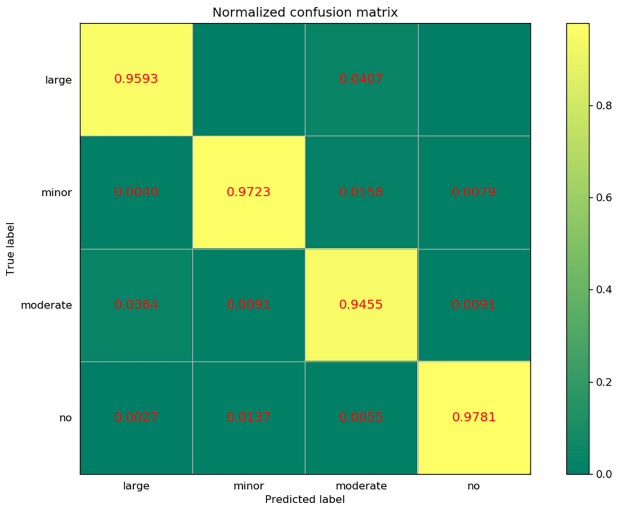

Fig. 7 Confusion matrix.

6 Conclusion

This paper proposed a CNN-based method to evaluate the leakage level of crude oil transmission pipes. The features automatically extracted from RGB images and thermal images were fused in the scoring stage of the proposed CNN model. By combining the RGB and thermal images, the method fully exploited the advantages of fusing the RGB images and thermal images. Experimental results verified that this fusion method outperformed other methods that use RGB images or thermal images alone.

References

[1] Gao, G. (2015). *Research on oil pipeline leak detection and location*. Master. Xi'an Shiyou University.

[2] Sinha, S. K. and Pandey, M.D. (2002). Probabilistic neural network for reliability assessment of oil and gas pipelines. *Computer - Aided Civil and Facilities Engineering*, 17(5), pp. 320-329.

[3] Ayello, F., Alfano, T., Hill, D. et al. (2012). A Bayesian network based pipeline risk management. In: *CORROSION*. Salt Lake City: NACE International, p. 14.

[4] Acciani, G., Brunetti, G., Fornarelli, G., et al. (2007). 3D-3 Classification of Defects for Guided Waves Inspected Pipes by a Neural Network Approach. In: *IEEE Ultrasonics Symposium Proceedings*. New York: IEEE, p. 4.

[5] Xiao, R., Hu, Q., and Li, J. (2019). Leak detection of gas pipelines using acoustic signals based on wavelet transform and Support Vector Machine. *Measurement*, 146, pp. 479-489.

[6] Guzman Urbina, A. and Aoyama, A. (2018). Pipeline risk assessment using artificial intelligence: A case from the colombian oil network. *Process Safety Progress*, 37(1), pp.110-116.

[7] Zhang, Z., Li, B., Lv, X. et al. (2018). Research on Pipeline Defect Detection Based on Optimized Faster R-cnn Algorithm. In: *International Conference on Applied Mechanics, Mathematics, Modeling and Simulation*. Hong Kong: AMMMS, p. 6.

[8] Sun, Y., Zuo, W., and Liu, M. (2019). Rtfnet: Rgb-thermal fusion network for semantic segmentation of urban scenes. *IEEE Robotics and Automation Letters*, 4(3), pp. 2576-2583.

[9] Ma, J., Ma, Y., and Li, C. (2019). Infrared and visible image fusion methods and applications: A survey. *Information Fusion*, 45, pp. 153-178.

[10] Khalid, B., Khan, A. M., Akram, M. U., et al. (2019). Person detection by fusion of visible and thermal images using convolutional neural network. In: 2019 2*nd International Conference on Communication, Computing and Digital systems (C-CODE)*. Islamabad: IEEE, pp. 143-148.

[11] LeCun, Y., Bottou, L., Bengio, Y. et al. (1998). Gradient based learning applied to document recognition. *Proceedings of the IEEE*, 86(11), pp. 2278-2324.

[12] Scherer, D., Müller, A. and Behnke, S. (2010). Evaluation of pooling operations in convolutional architectures for object recognition. Greece: *Springer Computer Proceedings*, pp. 92-101.

[13] Baldi, P. (1995). Gradient Descent Learning Algorithm Overview: A General Dynamical Systems Perspective. *IEEE Trans. Neural Networks*, 6(1), pp. 182-195.

[14] LeCun, Y., Kavukcuoglu, K. and Farabet, C. (2010). Convolutional networks and applications in vision. In: *IEEE International Symposium on Circuits and Systems*. Paris: IEEE, pp. 253-256.

[15] Wenku.baidu.com,(2017). *Basic knowledge of crude oil pipeline transportation*. [online] Available at: https://wenku.baidu.com/view/74faf8209a6648d7c1c-

708a1284ac850ad02043e. html [Accessed 27 May. 2018].

[16] Srivastava, N., Hinton, G. E., Krizhevsky, A., et al. (2014). Dropout: A Simple Way to Prevent Neural Networks from Overfitting. *Journal of Machine Learning Research*, 15(1), pp. 1929-1958.

Authors' Biographies

Anqi LI, received her B. S. degrees from Harbin Institute of Technology at Weihai, China, in 2017. She currently pursues her Master's degree, in Harbin Institute of Technology at Shenzhen (HITSZ). Her main research interest is mechatronic engineering.

E-mail: laqynl1030@126.com

Dongxu YE, received his B.S. degrees from Henan polytechnic University, China, in 2018. He currently pursues his Master's degree, in Harbin Institute of Technology at Shenzhen (HITSZ). His main research interest is mechatronic engineering.

E-mail: 1308848559@qq.com

Clarence W. de Silva, received Ph.D. degrees from Massachusetts Institute of Technology, Cambridge, MA, in 1978, and the University of Cambridge, Cambridge, U. K., in 1998, the Honorary D. Eng. degree from the University of Waterloo, Waterloo, ON, Canada, in 2008, and the higher doctorate, Sc. D., from the University of Cambridge, in 2020. He is a Professor of Mechanical Engineering at the University of British Columbia, Vancouver, BC, Canada, since 1988. His appointments include the Tier 1 Canada Research Chair in Mechatronics and Industrial Automation, Professorial Fellow, Peter Wall Scholar, Mobil Endowed Chair Professor, and NSERCBC Packers Chair in Industrial Automation. He has authored 25 books and about 560 papers, approximately half of which are in journals. His recent books, published by Taylor & Francis/CRC Press, include *Modeling of Dynamic Systems-With Engineering Applications* (2018), *Sensor Systems* (2017), *Sensors and Actuators – Engineering System Instrumentation*, 2nd Edition (2016), *Mechanics of Materials* (2014), *Mechatronics-A Foundation Course* (2010), *Modeling and Control of Engineering Systems* (2009), and *VIBRATION – Fundamentals and Practice*, 2nd Edition (2007); and by Addison Wesley, *Soft Computing and Intelligent Systems Design – Theory, Tools, and Applications* (with F. Karray, 2004).

Prof. de Silva is a Fellow of the American Society of Mechanical Engineers (ASME), the Institution of Electrical and Electronics Engineers (IEEE), the Canadian Academy of Engineering, and the Royal Society of Canada.

Email: desilva@mech.ubc.ca

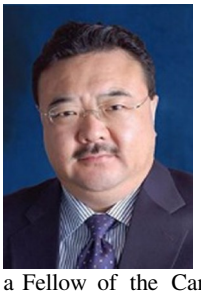

Max Q.-H. MENG, received PhD from University of Victoria (UVIC), Canada, in 1992. He is a Professor at the Chinese University of Hong Kong. He is currently the Chairman of the Department of Electrical Engineering at the Chinese university of Hong Kong. He is a Fellow of the Canadian Academy of Engineering and an IEEE fellow. His research interests include robotics, perception and AI with applications in medicine and services. He has published more than 600 journal and conference papers and book chapters and led more than 50 funded research projects to completion as PI.

E-mail: max.meng@cuhk.edu.hk